Carbohydrate Polymers 92 (2013) 1530–1538

Contents lists available at SciVerse ScienceDirect

Carbohydrate Polymers

journal homepage: www.elsevier.com/locate/carbpol

Dielectric studies of amylose, amylopectin and amylose–stearic acid complexes

Richard A. Pethrick*, Ma Song

WestChem, Department of Pure and Applied Chemistry, University of Strathclyde, 295 Cathedral Street, Glasgow G1 1XI, United Kingdom

ARTICLE INFO

Article history:
Received 26 June 2012
Received in revised form 20 August 2012
Accepted 24 September 2012
Available online 15 November 2012

Keywords:
Amylose
Amylopectin
Amylose–stearic acid complex
Dielectric relaxation
Protonic conduction

ABSTRACT

The effect of structure creation and moisture content on the dielectric properties of amylose, amylopectin and amylose–stearic acid complexes is presented. Three dielectric features have been identified in these systems. At low temperature, a dipole relaxation process is observed which is assigned to the reorientation of the —CH_2OH group. At ambient temperatures, a thermally activated relaxation is assigned to liberation–local chain motion. In certain systems at high temperatures, a Maxwell Wagner Sillars process is observed associated with the heterogeneous nature of media and is ascribed to the gel structure in the amylose–stearic acid complex. The low temperature relaxation is sensitive to the moisture content, the water molecules being bound to the —CH_2OH groups and the activation energy being reduced as the water content is increased. Comparison of the relaxation observed in amylose and amylopectin indicates that chain branching increases the activation energy and inhibits the local reorientation motion of the chain backbone. The relative magnitude of the relaxation processes and their activation energies are discussed in term of the structure of the polymer backbone, the nature of the complex formed with stearic acid and the extent to which order is created by thermal treatment. This paper gives insight into the changes in amylose mobility accompanying the formation of the various complexes.

1. Introduction

The existence of stable amylose–lipid complexes has been recognised for a number of years (Gidley, 1987; Gidley & Bociek, 1988; Morrison, 1988). Studies of a variety of food processing operations have revealed that the complexes can be formed as a result of many types of preparative operation (De Pilli, Derossi, Talja, Jouppila, & Severini, 2011; Exarhopoulos & Raphaelides, 2012; Tang & Copeland, 2007). Addition of fatty acids alters the physical and chemical properties of starchy foods and is attributed to the formation of the amylose and lipid complexes (De Pilli et al., 2008; Kaur & Singh, 2000; Nebesny, Rosicka, & Tkaczk, 2005; Singh, Cairns, Morris, & Smith, 1998). Stability of the complexes has been identified as an important factor in determining where digestion of the amylose and lipid occurs in the digestive track and this may have health implications (Kawai, Takato, Sasaki, & Kajiwara, 2012; Shelat, Vilaplana, Nicholson, Gidley, & Gilbert, 2011).

Amylose is present in all non-waxy starches and is essentially a linear homopolymer of linked-o-D-glucopyranose residues (De Pilli et al., 2008; Kaur & Singh, 2000; Nebesny et al., 2005; Singh et al., 1998). Three distinct polymorphs of amylose exist and are referred to as the A-, B- and V-forms and the V-form requires the presence of a complexing ligand. The A- and B-forms comprise parallel-packed, left-handed double helices (Imberty, Chanzy, Perez, Buleon, & Tran, 1988). Both these forms contain no internally bound water molecules, but they differ in the packing of the helices into bundles The A-form has a low and the B-form a higher level of water in the interstices. The A- and B-forms can be considered as extended helices with, unlike the V-form, no hydrogen bonding between consecutive turns of the helices. In the V-form, a single chain of amylose forms a helix with a relatively large cavity in which various ligands can be located and the number of glucosyl residues per turn (6, 7 or 8) depends on the ligand. The single V-helical complexes formed from a range of organic ligands and their structures have been reviewed (Gidley, 1987; Gidley & Bociek, 1988). The V-forms have relatively large central cavities with a pitch of about 8 Å per turn, whereas the double helical A- and B-forms have a pitch of about 21 Å and there is no internal cavity. X-ray diffraction (XRD), differential scanning calorimetry and NMR have been used to analyse melting transition characteristics and stability of the complexes (Waigh, Perry, Riekel, Gidley, & Donald, 1998; Jenkins & Donald, 1998; Jenkins et al., 1994; Morrison, Tester, Snape, Law, & Gidley, 1993; Morrison, 1988; Nebesny et al., 2005). The amylose–stearic acid complexes can exist in various forms depending on the conditions and temperature used in their formation (Gidley, 1987; Morrison, 1988; Morrison et al., 1993).

Dielectric characteristics of various forms of starch have reported (Butler & Cameron, 2000) and no significant differences were observed between a number of different types of starch.

* Corresponding author. Tel.: +44 01414 548 2795; fax: +44 0141 548 4822.
E-mail address: r.a.pethrick@strath.ac.uk (R.A. Pethrick).

0144-8617/$ – see front matter © 2012 Elsevier Ltd. All rights reserved.
http://dx.doi.org/10.1016/j.carbpol.2012.09.047

Several dielectric features were observed and attributed to rotation of methylol and short elements of the backbone.

Dielectric relaxation studies are able to reveal the extent to which dipole mobility is changed by the formation of molecular complexes and indicate the temperatures to which these structures must be raised in order that structural changes can occur. For thermally activated processes the temperature dependence of the relaxation frequency is directly related to the activation energy for conformational change. Enzyme attack and related chemical processes can be inhibited by the complex formation. Dielectric measurements will sense the reorientation of polar entities such as the OH and —O— linkages but will also provide information on the mobility of small molecules, such as water dispersed in the matrix. Whereas dynamic mechanical thermal analysis provides on the total chain dynamics and indicates the point at which large-scale motions become active, dielectric relaxation can sense the mobility of the individual dipoles. Dielectric measurements complement NMR studies, however, these latter measurements are difficult to interpret when the groups are hydrogen bonded.

2. Experimental

2.1. Materials

Amylose supplied by Sigma–Aldrich Chemical Company, UK was shown by X-ray analysis to be amorphous. The helix structure was obtained by retrograding amylose and the ^{13}C CP/MAS NMR was used to confirm that the helical structure was formed (Snape, Morrison, Maroto-Valer, Karkalas, & Pethrick, 1998). All the solvents used were analytical grade materials. The amylose as supplied was found to contain 10% H_2O and samples with different moisture content were created by heating a sample at 333 K for 4 h and 433 K for 2 h. A dry sample was also created by storing the material in a vacuum desiccator for 2 weeks over P_2O_5. The samples for measurement were prepared as 1.5 cm diameter disc with thickness typically between 0.05 and 0.1 cm^{-1} using 4000ypsi hydraulic press operated at room temperature.

2.2. Method to produce amylose–lipid complex

The stearic acid–amylose complex (Snape et al., 1998) was prepared using the alkaline route. Stearic acid was used as a model, as its complex with amylose is characteristic of those found with other lipids and it has been extensively investigated previously (Snape et al., 1998). Amylose solution in 0.01 M KOH was prepared using amylose–butanol complex and was mixed with a stearic acid solution in 0.01 M KOH at 358 K to give an amylose–stearic acid ratio by weight of 10/1. The complex was allowed to form at 333 K for 24 h. After three washes with water, the complex was freeze dried and followed by three washes with diethyl ether. The dry complex was re-dispersed in water.

The complex was reformed or recrystallised at 333 K and 363 K separately for 24 h and after dissociation at 423 K for 30 min to obtain form I and form II_l. Form II_l complex was annealed at 388 K for 24 h to obtain form II_h complex. All complexes were freeze dried and washed there times with diethyl ether to remove moisture.

As a reference, a 10% dispersion of stearic acid was prepared in hexatricontane (HC), which was obtained from Sigma–Aldrich UK. The mixture was heated to 353 K and a disc prepared and dielectric measurements performed.

2.3. Dielectric measurements

Measurements were performed using a Solartron 1250 frequency response analyser operating over a frequency range from 0.1 Hz to 6.3×10^5 Hz. A cell which consisted of two pre-etched copper electrodes mounted on an epoxy fibre glass substrate was created. The configuration used generates a three terminal electrode system with an active area of 1 cm^2. The sample discs were clamped between two electrodes and mounted on a heating block in a Oxford Instruments Cryostat (DN 1704). The electrodes were in good thermal contact and isothermal conditions were maintained using an Oxford Instruments ITC4 temperature controller. The method used has been described elsewhere (Hayward, Mahboubian Jones, & Pethrick, 1984). The temperature range studied was 150–440 K and measurements were performed at 10 K intervals. Data was recorded automatically and the frequency dependence of the real $\varepsilon'(\omega)$ and imaginary $\varepsilon''(\omega)$ permittivity calculated at each temperature.

The frequency dependence of the dielectric permittivity and loss was analysed using the Havriliak–Negami equation (Havriliak & Negami, 1967):

$$\varepsilon^*(\omega) = \varepsilon_\infty + \frac{\Delta\varepsilon}{(1 + (i\omega\tau)^\alpha)^\beta} \quad (1)$$

where $\varepsilon^*(\omega)$ is the frequency (ω) dependent complex dielectric permittivity, related to the real dielectric permittivity $\varepsilon'(\omega)$ and dielectric loss $\varepsilon''(\omega)$ by $\varepsilon^*(\omega) = \varepsilon'(\omega) + i\varepsilon''(\omega)$ and τ is the characteristics relaxation time for the dipole relaxation process, $\Delta\varepsilon$ is the dielectric increment associated with the relaxation, α and β are distribution parameters describing the breadth of the relaxation process. The magnitude of $\Delta\varepsilon$ is related to $\varepsilon_0 - \varepsilon_\infty$ the difference between the low ε_0 and high frequency ε_∞ limiting values associated with the dipolar relaxation process. The experimental data were fitted to Eq. (1), separated into its real and imaginary parts using a MathCAD programme. Variation of τ with temperature allows calculation of the activation energy from Arrhenius plots of the relaxation data.

3. Results and discussion

3.1. Low temperature relaxations

In order to interpret the dielectric studies on the amylose–stearic acid complex, measurements were first performed on amylose, amylopectin and stearic acid. Moisture can interact with the amylose and plays an important part in determining its structure. Samples were prepared with different levels of moisture and the results are presented in Figs. 1–3. The high moisture content sample was obtained by heating the sample at 333 K for 4 h and had a moisture content of 4%. The middle

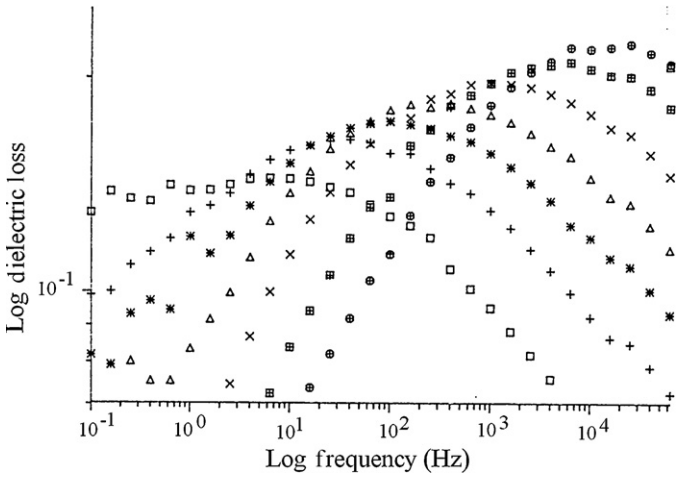

Fig. 1. Dry amylose. *Key*: □, 170 K; +, 180 K; ⊠, 190 K; △, 200 K; ×, 210 K; ⊞, 220 K; ⊕, 230 K.

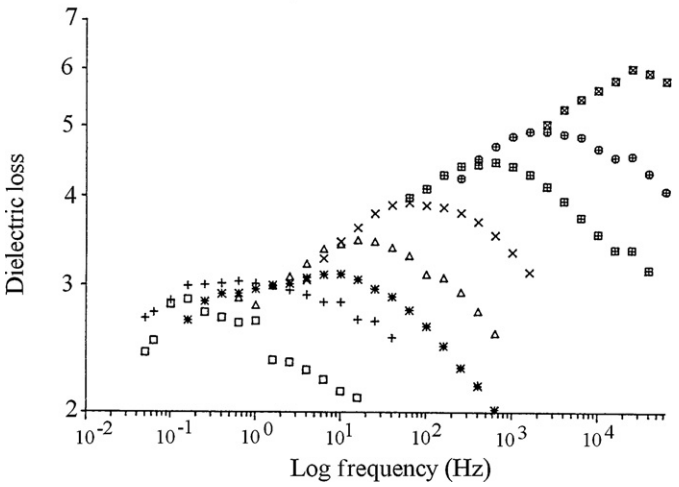

Fig. 2. Middle moisture amylose (~1%). *Key*: □, 170 K; +, 180 K; ⊠, 190 K; △, 200 K; ×, 210 K; ⊞, 220 K; ⊕, 230 K.

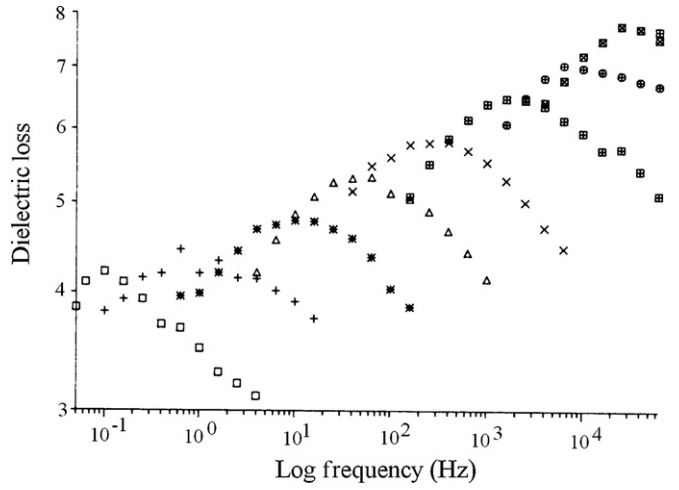

Fig. 3. High moisture content amylose (4%). *Key*: □, 170 K; +, 180 K; ⊠, 190 K; △, 200 K; ×, 210 K; ⊞, 220 K; ⊕, 230 K.

moisture content sample was obtained by drying in an oven overnight at 353 K and the moisture content was ~1%. The dry sample was obtained by drying over P_2O_5 in a vacuum desiccator for more than 2 weeks, the moisture content being undetectable.

The Havriliak–Negami analysis of the curve indicates that at all moisture contents the value of β is close to unity, varying from 0.9 to 0.98 in the case of the highest moisture content. A value

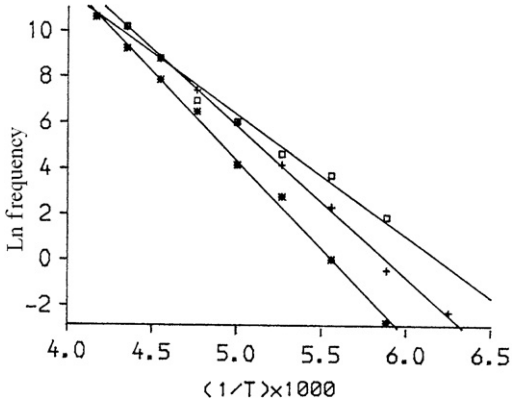

Fig. 4. Plot of the variation of the ln(relaxation frequency) versus $1/T$ for the 4% moisture (□), the 1% moisture (+) and dry (⊠) amylase materials.

approximately of unity indicates that the low temperature is a single dipole relaxation process which is broadened as the temperature is increased reflected in that values of α which vary from 0.77 to 0.56 (Table 1). The value of α indicates spread of environments experienced by the relaxing dipoles and the number and distribution of hydrogen bonding sites involved in defining the rotational potential surface. The variation of the relaxation frequency versus $1/T$ shows a linear variation indicative of a thermally activated process and the slope allows the Arrhenius activation energy for the process to be calculated (Fig. 4). Increasing the moisture content leads to an increase in the amplitude of the dielectric relaxation process; $\varepsilon'_{max} - \varepsilon'_{min}$ increasing from a value of ~1.5 in the dry sample, to a value of ~2.1 in the 1% moisture content material and further increasing to ~4.8 in the 4% moisture content sample. The dielectric permittivity of water of 80 and 4% moisture content would increase the dielectric permittivity by 3.2. The base permittivity, ε'_0, of the dry sample is 1.5 which would raise ε'_0 to a value of 4.8, consistent with observed on the addition of 4% moisture. The relaxation in the dry sample is attributed to the relaxation of the $-CH_2OH$ dipole of the glycoside entity (Butler & Cameron, 2000; Einfeldt, Kwasniewski, Klemm, Dicke, & Einfeldt, 2000) and the above observations would support this proposition. The additional increment to $\varepsilon'_{max} - \varepsilon'_{min}$ in the moist samples can be associated with water molecules interacting with the amylose–CH_2)H pendant groups. The activation energy of the dry sample is 62.6 kJ mol^{-1} and decreases to 45.1 kJ mol^{-1} when the hydration level is increased to 1% and drop to 43.1 kJ mol^{-1} when the hydration level is increased to 4%. The activation energy for the $-CH_2OH$ rotation has previously been reported (Einfeldt et al., 2000; Kaminski et al., 2009; Ramasamy, 2012) with values between 48 and 51 kJ mol^{-1} for cellulose. Lowering of the activation energy

Table 1
Analysis of the dielectric spectra for of amylase in varying states of hydration.

Temperature (K)	ε'_{min}	ε'_{max}	$\varepsilon'_{max} - \varepsilon'_{min}$	α	β	ε''_{max}
Dry retrograded amylose						
220	3.05	5.95	2.90	0.74	0.90	0.29
230	3.00	6.06	3.06	0.70	0.80	0.32
240	3.40	6.14	2.74	0.67	0.90	0.32
250	3.0	6.34	3.34	0.71	0.90	0.37
260	3.10	6.40	3.30	0.68	0.90	0.41
Dry amylopectin						
150	1.91	2.70	0.79	0.74	0.90	0.075
160	1.95	2.62	0.67	0.69	0.90	0.080
170	1.94	2.68	0.74	0.70	0.90	0.085
180	1.98	2.64	0.66	0.68	0.90	0.90
190	2.00	2.70	0.70	0.66	0.90	0.09
200	1.92	2.74	0.82	0.69	0.90	0.10

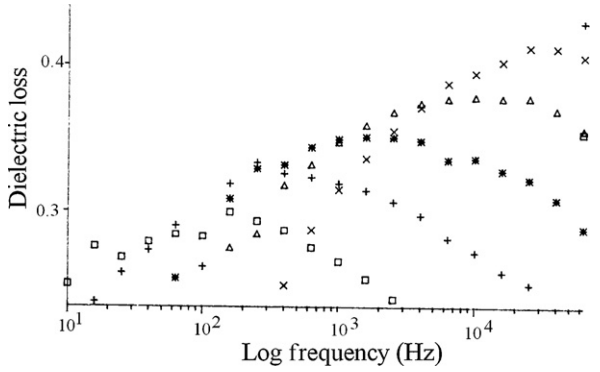

Fig. 5. Dielectric loss for dry retrograded amylose. *Key*: □, 170 K; +, 180 K; ⊠, 190 K; △, 200 K; ×, 210 K; ⊞, 220 K; ⊕, 230 K.

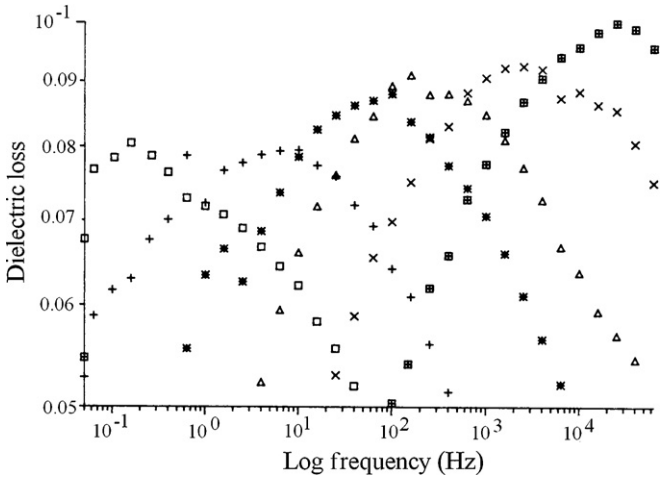

Fig. 6. Dielectric loss for dry amylopectin. *Key*: □, 170 K; +, 180 K; ⊠, 190 K; △, 200 K; ×, 210 K; ⊞, 220 K; ⊕, 230 K.

with increased moisture content reflects the change in the nature of the hydrogen bonding constraining free rotation of the $-CH_2OH$ groups in the amylose and the plasticisation effect of the added water on the relaxation process.

3.2. Retrograded amylose

The retrograded amylose is a crystalline double helix structure and may be expected to influence the relaxation of the $-CH_2OH$ dipole. The low temperature dielectric loss for the dry retrograded amylose, Fig. 5 is similar to that for the less ordered material, Fig. 1, but the analysis of the spectrum reveals distinct differences (Table 2). Conversion of the less ordered amylose to the retrograded form increased the value of dielectric increment from ~1.55 to and value of ~3.0. In the case of plastic crystals, an increase in the dielectric increment is observed with the creation of a more ordered environment for the dipole relaxation (Clemett & Davies, 1962). The creation of an ordered backbone structure aides the development of a better defined potential energy surface but also increases the activation energy from 62.6 kJ mol^{-1} for the amorphous material to 65.4 kJ mol^{-1} for the retrograded form. In the amorphous material the disorder in the structure will allow a range of different inter atomic distances to exist which will influence the potential energy surface which will be simplified by the creation of a more regular-ordered structure.

3.3. Amylopectin

The dielectric behaviour of dry amylopectin was investigated (Fig. 6). The sample used in this study was derived from waxy starch and has a crystallinity of ~30%. Amylopectin has a significantly more disordered structure than either amylose or retrograded amylose and the result on the dielectric spectrum is a significant reduction in the observed amplitude of the relaxation. The amplitudes in the amylopectin being reduced to a value of ~0.7 for $\varepsilon'_{max} - \varepsilon'_{min}$ compared with values of ~3.0 and 1.5 for, respectively, the ordered retrograded amylose and amylose. The disordered structure will allow hydrogen bonding with a variety of different sites and there will be a general opening up of the structure and this is reflected in a lowering of the activation energy to a value of 53.9 kJ mol^{-1}.

Table 2
Analysis of the dielectric spectra for dry retrograded amylose and amylopectin.

Temperature (K)	ε'_{min}	ε'_{max}	$\varepsilon'_{max} - \varepsilon'_{min}$	α	β	ε''_{max}
Amylose relaxation II						
320	5.5	13.0	7.5	0.22	0.98	2.5
330	5.5	15.3	9.8	0.22	0.98	3.5
340	5.5	17.0	11.7	0.26	0.95	3.7
350	5.5	18.8	13.4	0.31	0.95	3.9
360	5.5	19.5	14.0	0.30	0.95	4.1
370	5.6	19.2	13.7	0.30	0.95	4.1
380	5.7	20.0	14.3	0.29	0.95	4.2
390	5.8	19.0	13.2	0.28	0.95	4.3
Amylose relaxation III						
400	13.0	117	104	0.35	0.95	28.6
410	13.0	175	162	0.30	0.95	47.4
420	12.0	267	255	0.32	0.95	73.0
430	14.0	355	341	0.31	0.95	100
440	15.0	475	460	0.30	0.95	140
Amylopectin (dry)						
340	2.78	3.33	0.55	0.28	0.90	0.17
350	2.80	3.43	0.63	0.27	0.90	0.20
360	2.81	3.51	0.70	0.28	0.90	0.22
370	2.82	3.52	0.70	0.28	0.90	0.22
380	2.83	3.53	0.70	0.28	0.90	0.22
390	2.87	5.55	0.68	0.25	0.90	0.22
400	3.15	3.87	0.72	0.27	0.90	0.22
410	3.41	4.25	0.84	0.33	0.90	0.23
420	3.60	4.40	0.80	0.30	0.90	0.23

Table 3
Analysis of the dielectric spectra for the high temperature processes in amylose and amylopectin.

Temperature (K)	ε'_{min}	ε'_{max}	$\varepsilon'_{max} - \varepsilon'_{min}$	α	β	ε''_{max}
Amylose relaxation II						
320	5.5	13.0	7.5	0.22	0.98	2.5
330	5.5	15.3	9.8	0.22	0.98	3.5
340	5.5	17.0	11.7	0.26	0.95	3.7
350	5.5	18.8	13.4	0.31	0.95	3.9
360	5.5	19.5	14.0	0.30	0.95	4.1
370	5.6	19.2	13.7	0.30	0.95	4.1
380	5.7	20.0	14.3	0.29	0.95	4.2
390	5.8	19.0	13.2	0.28	0.95	4.3
Amylose relaxation III						
400	13.0	117	104	0.35	0.95	28.6
410	13.0	175	162	0.30	0.95	47.4
420	12.0	267	255	0.32	0.95	73.0
430	14.0	355	341	0.31	0.95	100
440	15.0	475	460	0.30	0.95	140
Amylopectin (dry)						
340	2.78	3.33	0.55	0.28	0.90	0.17
350	2.80	3.43	0.63	0.27	0.90	0.20
360	2.81	3.51	0.70	0.28	0.90	0.22
370	2.82	3.52	0.70	0.28	0.90	0.22
380	2.83	3.53	0.70	0.28	0.90	0.22
390	2.87	5.55	0.68	0.25	0.90	0.22
400	3.15	3.87	0.72	0.27	0.90	0.22
410	3.41	4.25	0.84	0.33	0.90	0.23
420	3.60	4.40	0.80	0.30	0.90	0.23

In all the systems studied the dipole relaxation reflects a distribution of sites contributing to the overall relaxation as signified by a value of α of ~0.7. If the dipole relaxation was a simple reorientation process then the values of α and β would be expected to have values of unity. Deviations from unity are indicative of a distribution of relaxation sites. In all theses systems, the dipolar relaxation occurs in the same temperature–frequency window and therefore can be assumed to have similar origins. The rotation of the —CH_2OH dipole will involve breaking and making of new hydrogen bond interactions and will be coupled to the mobility of other entities on the structure.

3.4. High temperature relaxation

As reported by other workers (Butler & Cameron, 2000; Kaminski et al., 2009) dielectric relaxation processes are observed at high temperature and are attributed to local motion of the chain backbone. However, close examination of the dielectric loss plots indicates that there is a significant contribution from ionic conductivity which masks the process the weaker dipole processes. However, since the d.c. conductivity does not add to the dielectric permittivity it does not influence the permittivity plots (Fig. 6).

The dielectric spectrum can be resolved into two processes for both amylose and retrograded amylose. The results of the analysis are presented in Table 3. The highest temperature relaxation amylose III process, Table 3, has a large amplitude which is inconsistent with a dipole relaxation process and must be ascribed to polarisation effects associated with the heterogeneity of the material. This so called Maxwell Wagner Sillars process, has been observed in a wide range of heterogeneous materials (North, Pethrick, & Wilson, 1978) and arises from the trapping of mobile charge carriers at interfaces within the material. The charge carriers in amylose and amylopectin must arise form the ionisation of either residual water molecules or alternately the pendant hydroxyl groups. If these are able to interact down the chain then conduction can be achieved using a Grotthuss type of mechanism in which proton injection at one point allows facile transport to a more distant location (Fig. 7).

The activation energy for this high temperature process is 107.8 kJ mol^{-1}. The proton conduction will require in the dry materials support proton conduction and this will involve hopping of the charge between neighbouring sites and will be expected to have a high activation energy. The relaxation process observed at intermediate temperatures has an activation energy of 79.3 kJ mol^{-1}, which is higher than that for the lower temperature process and is consistent with the process being associated with a restricted local reorientation of the polymer backbone (Einfeldt et al., 2000; Tylianakis, Spyros, Dais, Taravel, & Perico, 1999). The local motion of the backbone is assumed to involve motion of the OH dipoles and liberation motion of the —O— linkages and has a significantly higher a value for ε''_{max} of 4.0 compared with the lower temperature value of ~0.2. Other workers (Butler & Cameron, 2000; Kaminski et al., 2009) have assigned relaxations in this region to local motions of the chain backbone which will be a high coupled processes and consistent with the breadth of the relaxation described by a value of α of ~0.2–0.3 being significantly less than that form the —CH_2OH relaxation with α ~0.7.

Cooperative motions do occur in a carbohydrate chain (Tylianakis et al., 1999). Conformational transitions in a carbohydrate chain are not completely isolated events. However, the nature and the extent of these cooperative motions in a carbohydrate chain are different from those associated with the glass transition

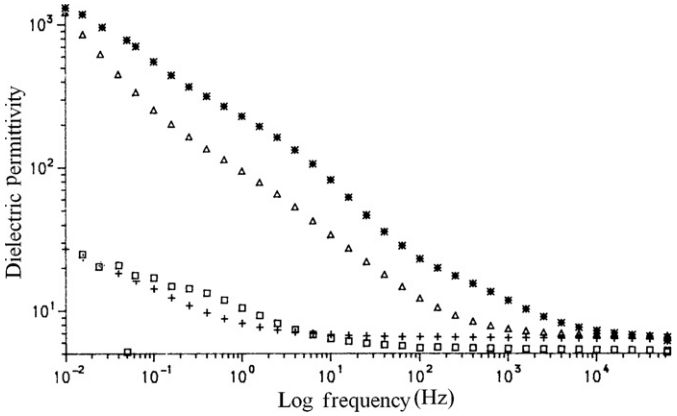

Fig. 7. Dielectric permittivity for □, amorphous amylose at 340 K; +, retrograded amylose at 340 K; ⊞, amorphous amylose at 420 K; △, retrograded amylose at 420 K.

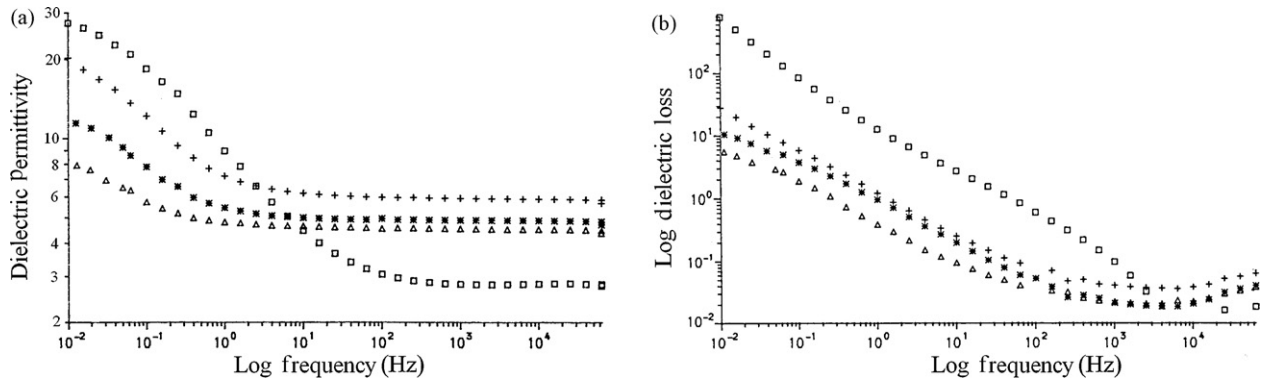

Fig. 8. Dielectric permittivity [*A*] and loss [*B*] for stearic acid in various environments. *Key*: □, stearic acid in HC; +, amylose–stearic acid type I complex; ⊠, amylose–stearic acid complex form at 90 °C (II_l); △, amylose–stearic acid complex formed at 115 °C (II_h).

in hydrocarbon backbone of elements of the glucosidic ring and the ether linkages.

The relaxation behaviour of the amylopectin is significantly different from that of the amylose, the value of ε''_{max} is significantly smaller at ~0.22, however, the activation energy is 51.9 kJ mol^{-1} which is comparable with that in amylose. The reduction in amplitude is a reflection of the branched chains inhibiting the motion and reducing the proportion of the chain which can be involved in this type of motion.

The high frequency limiting values of ε'_∞ has value which is simply the sum of the contribution due to the polymer lattice and an additional contribution from the $-CH_2OH$ dipole and there is no indication of relaxation processes associated with water, consistent with the contention that the amylose structure excludes water from the internal helix structure.

3.5. Amylose–stearic acid complexes

3.5.1. High temperature dielectric behaviour

The complexes studied were created using a 10:1 ratio of amylose and stearic acid and subsequent heat treatment of the initially formed type I complex to form the II_l and II_h forms was carried out. Stearic acid has the potential of exhibiting dielectric relaxation and it is therefore appropriate to firstly characterise its relaxation behaviour. In order to reduce the effects of protonic conduction on the dielectric measurements, stearic acid was studied as a 10% dispersed in non-polar hexatriacontane (HC). The concentration of stearic acid was maintained constant in all the samples examined allowing direct comparison between the relaxation processes observed. The traces obtained at two temperatures; 340 K, Fig. 8 and 420 K Fig. 9 are presented. Stearic acid is a crystalline solid at room temperature and has a melting point of 340 K. In the presence of the electric field ionisation can occur:

$$RCOOH \longrightarrow RCOO^{\ominus} + H^{\oplus}$$

The stearic acids in HC is demonstrating a high dielectric loss at <10^3 Hz which is typical of the MWS process observed in a phase separated media. In the HC, small clusters of stearic acid will through protonic conduction within the microcrystallites produce a large contribution to the dielectric constant, Fig. 8A and loss Fig. 8B. In both the stearic acid dispersion in HC and the amylose–stearic acid complexes, the ionic conductivity is significantly greater than in the studies of amylose or amylopectin. In the former systems, conduction requires hopping between neighbouring OH sites arises whereas in these stearic acid containing systems ionisation of the carboxyl group can increase the concentration of charge carriers and hence the level of ionic conduction.

The dielectric loss, $\varepsilon''(\omega)$, exhibits the characteristic $1/\omega$ dependence of a system with a significant level of d.c. conductivity. The amylose–stearic acid complex is known to solids which contain 20% torus/disc species and 80% of a lobed species (Fanta, Felker, Shogren, & Salch, 2006; Kawai et al., 2012). The MWS process reflects the size and shape of the structures formed (North et al., 1978) and the breadth of the relaxation, Table 4, which is of the order of 0.2–0.33, indicate that the structures have more than one form, consistent with the previous electron microscopic observations (Fanta et al., 2006). The amplitude of the process will be influenced by the ionic mobility in the system, as well as the type of structure and its alignment. The amylose–stearic acid complexes exhibit both lower level of the permittivity and dielectric loss then the dispersion of stearic acid. The incorporation of the stearic acid within the amylose helix

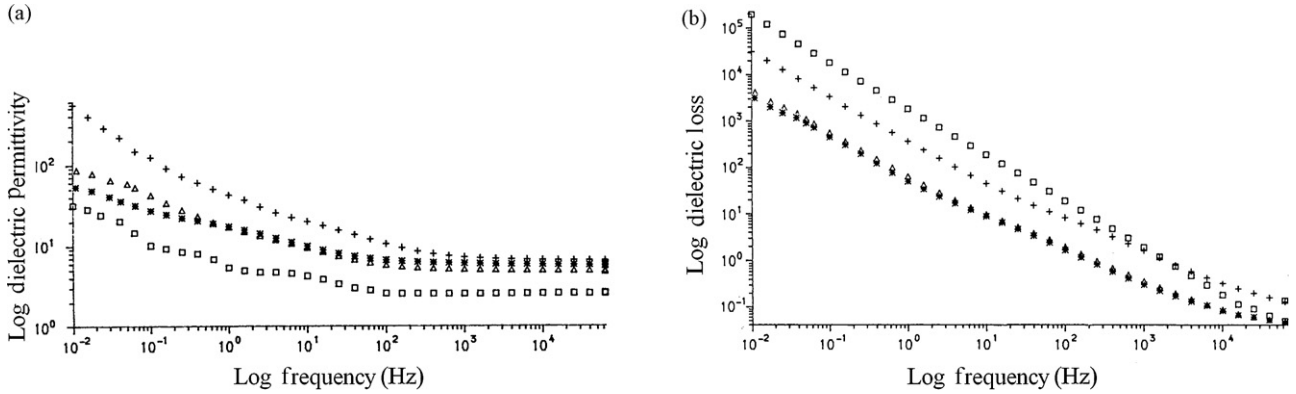

Fig. 9. Dielectric permittivity [*A*] and loss [*B*] for stearic acid in various environments. *Key*: □, stearic acid in HC; +, amylose–stearic acid type I complex; ⊠, amylose–stearic acid complex form at 90 °C (II_l); △, amylose–stearic acid complex formed at 115 °C (II_h).

Table 4
Dielectric parameters for the high temperature dielectric relaxation in amylose–stearic acid complexes.

Temperature (K)	ε'_{min}	ε'_{max}	$\varepsilon'_{max} - \varepsilon'_{min}$	α	β	ε''_{max}
Amylose stearic acid complex type I						
340	5.68	7.37	1.51	0.39	0.90	0.37
350	5.89	7.50	1.61	0.33	0.90	0.44
360	6.00	8.15	2.15	0.35	0.90	0.58
370	5.15	8.90	2.75	0.28	0.90	0.82
380	6.20	9.12	2.92	0.29	0.90	0.88
390	6.25	10.08	3.83	0.33	0.90	1.06
400	6.36	10.46	4.10	0.33	0.90	1.14
Amylose stearic acid complex type II_l						
340	4.90	6.18	1.28	0.25	0.90	0.40
350	4.91	6.48	1.57	0.34	0.90	0.44
360	4.95	6.44	1.49	0.32	0.90	0.44
370	5.05	6.62	1.57	0.31	0.90	0.45
380	4.16	6.90	1.74	0.29	0.90	0.50
390	5.29	7.27	1.98	0.35	0.90	0.54
400	5.71	8.09	2.38	0.30	0.90	0.69
410	8.08	8.96	2.88	0.28	0.90	0.87
420	6.20	9.64	3.44	0.24	0.90	1.10
430	6.20	10.52	4.32	0.23	0.90	1.40
Amylose stearic acid complex type II_h						
350	4.66	5.88	1.22	0.37	0.90	0.32
360	4.70	6.58	1.88	0.36	0.90	0.48
370	4.82	7.68	2.86	0.28	0.90	0.86
380	4.92	8.36	3.44	0.21	0.90	1.16
390	5.01	9.50	4.49	0.22	0.90	1.50
400	5.27	10.6	5.33	0.20	0.90	1.80
410	5.32	11.5	6.18	0.20	0.90	2.10

effectively removes its contribution to the conduction and reduces the MWS losses by decreasing the ionic mobility. The more perfect the structure, the lower the ionic mobility and hence the amplitude of the relaxation. Heat treatment of the complex increasing the perfection and reduces the mobility of the stearic acid. The magnitude of the dielectric permittivity falls in the order type I, type II_l to type II_h and reflects the increasing perfection of the complex as a consequence of the heat treatment.

The high frequency permittivity drops to a low value ~2.5 in the case of the stearic acid mixture, which is approximately the value of the refractive index squared and indicates that there are no further processes occurring at higher frequency. In the case of the amylose–stearic acid complexes, the limiting value is higher ~6 in the type II complex and is reduced to a value of ~5 in the type II_h complex. In these systems there will still remain at higher frequency dipole relaxation associated with the reorientation of the $-CH_2OH$ groups and librational motion of the chain backbone. The value of the limiting value of ε'_∞ is consistent with the proposition that water is excluded form within the amylose helix. As the perfection of the complex is improved so the extent to which these groups can partake in the relaxation will be reduced and this is reflected in a corresponding reduction in the high frequency limiting value.

Amylose–stearic acid complex type I was formed at 333 K and has a melting temperature of about 371 K. X-ray diffraction shows that the type I complex is composed of nearly random V-helices, while type II_l and type II_h are typically partially crystalline (Exarhopoulos & Raphaelides, 2012). The type I complex is composed of nearly random V-helices, whereas the type II complexes V-helices form crystalline domains which will be dispersed in more amorphous material. The dielectric relaxation in terms of the MWS relaxation is consistent with the complex having a gel like morphology. The relative reduction in the high frequency limiting values of the dielectric permittivity is consistent with the observation the retrograded amylose shows a reduced dielectric activity relative to the more disordered form of the structure. The relaxation analysed using Eq. (1) and the values of the constants obtained are summarised in Table 4. Plots of the temperature dependence of the relaxation frequency, Fig. 10, can be fitted to an Arrhenius equation consistent of the thermally activated relaxation process and yield values of the activation energy of amylose–stearic acid complex type I of 72.3 kJ mol^{-1} which is reduced to 55.8 kJ mol^{-1} for type II_l and is further reduced to 51.9 kJ mol^{-1} in type II_h.

The amylose–stearic acid complex has the carboxyl group incorporated into the helix (Le Bail, Buleon, Shiftan, & Marchessault, 2000; Le Bail, Rondeau, & Buleon, 2000; Shelat et al., 2011) and the complexation with the amylose appears to assist the ionisation of the proton which controls the activation energy for the MWS process. The more perfectly the head group is bound into the helix the easier the ionisation of the COOH group.

3.5.2. Low temperature relaxation behaviour

As in the case of amylose, the amylose–stearic acid complex exhibits a dielectric relaxation at low temperatures (Fig. 11). The dielectric response of the three types of the amylose–stearic acid complex exhibit slightly different relaxation features. Type I, Figure 8A, exhibits a variation in amplitude with temperature

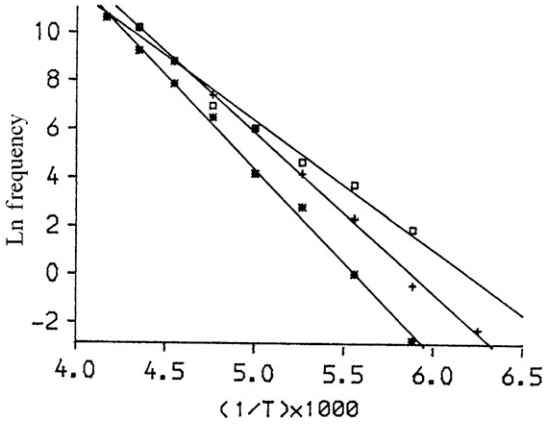

Fig. 10. Plot of the ln of the relaxation frequency against reciprocal temperature for the higher temperature relaxation in the amylose–stearic acid complex. *Key*: □, amylose–stearic acid type I complex; +, amylose–stearic acid complex form at 90 °C (II_l); ⊠, amylose–stearic acid complex formed at 115 °C (II_h).

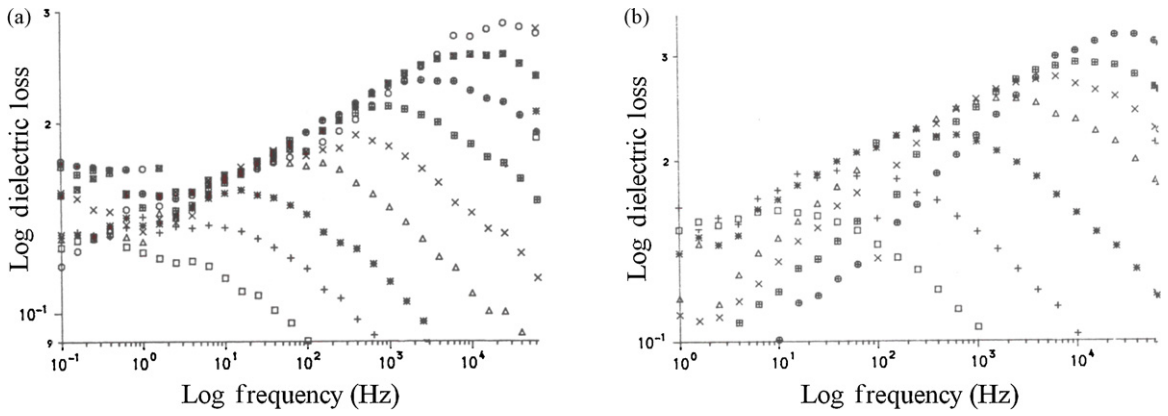

Fig. 11. Dielectric loss for amylose–stearic acid complex *t* [*A*] type I, [*B*] type II_l and [*C*] type II_h. *Key*: □, 170 K; +, 180 K; ⊠, 190 K; △, 200 K; ×, 210 K; ⊞, 220 K; ⊕, 230 K.

Table 5
Dielectric parameters for the low temperature dielectric relaxation in amylose–stearic acid complexes.

Temperature (K)	ε'_{min}	ε'_{max}	$\varepsilon'_{max} - \varepsilon'_{min}$	α	β	ε''_{max}
Amylose stearic acid complex type I						
150	3.05	4.50	1.45	0.77	0.90	0.13
160	3.08	4.40	1.32	0.73	0.90	0.14
170	3.10	4.50	1.40	0.72	0.90	0.15
180	3.10	4.64	1.54	0.71	0.90	0.17
190	3.10	4.84	1.74	0.71	0.90	0.19
200	3.08	4.96	1.88	0.71	0.90	0.21
210	3.05	5.16	2.11	0.72	0.98	0.23
220	2.98	5.30	2.32	0.72	0.95	0.25
Amylose stearic acid complex type II_l						
170	2.52	3.92	1.40	0.69	0.90	0.17
180	2.56	4.06	1.50	0.67	0.90	0.18
190	2.51	4.40	1.89	0.70	0.90	0.22
200	2.40	4.68	2.28	0.70	0.85	0.25
210	2.40	4.60	2.20	0.64	0.80	0.28
220	2.55	4.72	2.17	0.65	0.90	0.29
230	2.52	4.89	2.37	0.65	0.90	0.32
Amylose stearic acid complex type II_l						
170	2.35	3.47	1.12	0.70	0.90	0.13
180	2.34	3.56	1.22	0.70	0.90	0.14
190	2.34	3.68	1.34	0.70	0.90	0.15
200	2.35	3.77	1.42	0.68	0.90	0.17
210	2.33	3.90	1.57	0.69	0.90	0.19
220	2.34	3.97	1.63	0.67	0.90	0.21
230	2.33	4.06	1.73	0.66	0.90	0.23

which is similar to that found in amylose. A similar pattern is found in type II_l and type II_h but the amplitude of the loss is slightly reduced as the perfection of the structure is increased, Fig. 11B and C. The dielectric data can be analysed using Eq. (1) and the results are presented in Table 5.

The distribution parameters, α and β indicate that the relaxation is significantly narrower than the high temperature process and that values are similar to those observed in amylose. The values of $\varepsilon'_{max} - \varepsilon'_{min}$ and ε''_{max} exhibit small differences between the complexes and reflect the effects of change in the structure on the relaxation process. The variation of the relaxation frequency with reciprocal temperature, Fig. 12 allows determination of the Arrhenius activation energy which for the low temperature type I complex is 41.5 kJ mol^{-1}, complex type II_l is 44.2 kJ mol^{-1} and complex type II_h is 40.7 kJ mol^{-1}.

The activation energy is lower than that observed in the dry amylose and is more comparable to that of the samples which contained moisture. However, if we assume that the relaxing dipole is that of the $-CH_2OH$ group then a lower activation energy would be consistent with changes in the binding of this group to its neighbours as a consequence of the accommodation within the helix of the stearic acid, which is in agreement with X-ray structural studies on these materials (Exarhopoulos & Raphaelides, 2012).

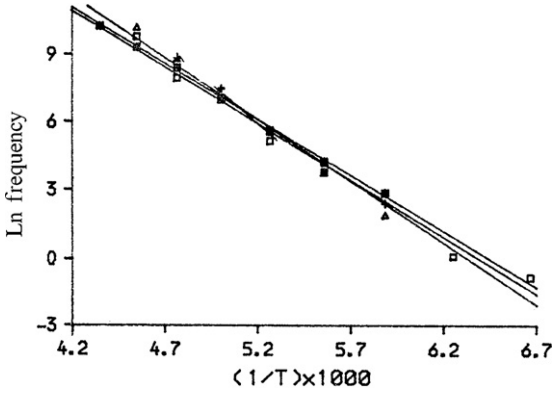

Fig. 12. Plot of ln frequency against reciprocal temperature for the low temperature relaxation *Key*: □, amylose–stearic acid type I complex; +, amylose–stearic acid complex form at 90 °C (II_l); ⊠, amylose–stearic acid complex formed at 115 °C (II_h).

4. Conclusions

The dielectric measurements for both the amylose, amylopectin and the amylose–stearic acid complex conform too

thermally activated dipolar processes; at low temperatures, the reorientation of the CH_2OH group which will be located on the outside of the helical backbone structure and librational–local rotational motion of the backbone at higher temperatures. The activation energy varies with changes in the structure of the polymer backbone reflecting the variation in the nature of the hydrogen bonding around the relaxation site and implying a relatively small number of chain elements are involved. Increasing the degree of hydration loosens the hydrogen bond interactions and lowers the activation energy. Heat stabilisation of the amylose–stearic acid complex increases the perfection of the helical structure and this is observed as changes in the form of the dielectric relaxation. Theses observations are in agreement with measurements of the mechanical properties where the storage modulus is inferred as reflecting local motions of the chain (Kasapis, 2012). The highest temperature relaxation process has the form of an MWS process and the existence of micro phase structures is in agreement with the electron microscopic observation of the complexes having a range of different shapes (Fanta et al., 2006; Kawai et al., 2012).

Acknowledgement

One of us (MS) wishes to acknowledge the support of EPSRC in terms of a post-doctoral fellowship for the period of this study.

References

Butler, M. F., & Cameron, R. E. (2000). A study of the molecular relaxation in solid starch using dielectric spectroscopy. *Polymer*, *41*, 2249–2262.

Clemett, C., & Davies, M. (1962). Dielectric relaxation studies of rotator phase solids. 2. Camphane derivatives. *Transactions of the Faraday Society*, *58*(477), 1718–1723.

De Pilli, T., Derossi, A., Talja, R. A., Jouppila, K. C., & Severini, C. (2011). Study of starch-lipid complexes in model system and real food produced using extrusion-cooking technology. *Innovative Food Science and Emerging Technologies*, *12*, 610–616.

De Pilli, T., Jouppila, K., Ikonen, J., Kansikas, J., Derossi, A., & Severini, C. (2008). Study on formation of starch-lipid complexes during extrusion-cooking of almond flour. *Journal of Food Engineering*, *87*, 495–504.

Einfeldt, J., Kwasniewski, A., Klemm, D., Dicke, R., & Einfeldt, L. (2000). Analysis of side group motion in O-acetyl-starch using regioselective 2-O-acetyl-starches by means of dielectric spectroscopy. *Polymer*, *41*, 9273–9281.

Exarhopoulos, S., & Raphaelides, S. N. (2012). Morphological and structural studies of thermally treated starch-fatty acid systems J. *Cereal Science*, *55*, 139–152.

Fanta, G. F., Felker, F. C., Shogren, R. L., & Salch, J. H. (2006). Effect of fatty acid structure on the morphology of spherulites formed from jet cooked mixtures of fatty acids and defatted corn starch. *Carbohydrate Polymers*, *66*, 60–70.

Gidley, M. (1987). Factors affecting the crystalline type (AC) of native starches and model compounds – A rationalization of observed effects in terms of polymorphic structures. *Carbohydrate Research*, *161*(2), 301–304.

Gidley, M., & Bociek, S. M. (1988). C-13 CP/MAS NMR-studies of amylose inclusion complexes, cyclodextrins, and the amorphous phase of starch granules – Relationships between glycosidic linkage. *Journal of the American Chemical Society*, *110*(12), 3820–3829.

Hayward, D., Mahboubian Jones, B. G., & Pethrick, R. A. (1984). Low-frequency dielectric measurements (10^{-4} to 6×10^4 Hz) – A new computer-controlled method. *Journal of Physics Part E: Scientific Instruments*, *17*(8), 683–690.

Havriliak, S., & Negami, S. (1967). A complex plane representation of dielectric and mechanical relaxation processes in some polymers. *Polymer*, *8*, 161–210.

Imberty, A., Chanzy, H., Perez, S., Buleon, A., & Tran, V. (1988). The double-helical nature of the crystalline part of A-starch. *Journal of Molecular Biology*, *201*(2), 365–378.

Jenkins, P. J., Cameron, R. E., Donald, A., Bras, W., Derbyshire, G. E., Mant, G. R., et al. (1994). In situ simultaneous small and wide angle X-ray scattering: A new technique to study starch gelatinization. *Journal of Polymer Science Part B: Polymer Physics*, *32*, 1579–1585.

Jenkins, P. J., & Donald, A. M. (1998). Gelatinization of starch: A combined SAXS/WAXS/DSC and SANS study. *Carbohydrate Research*, *308*, 133–147.

Kaminski, K., Kaminska, E., Ngai, K. L., Paluch, M., Wlodarczyk, P., Kasprzycka, A., et al. (2009). Identifying the origins of two secondary relaxations in polysaccharides. *Journal of Physical Chemistry B*, *113*, 10088–10096.

Kasapis, S. (2012). The relation between the structure of matrices and their mechanical relaxation mechanism during the glass transition of biomaterials: A review. *Food Hydrocolloids*, *26*, 464–472.

Kaur, K., & Singh, N. (2000). Amylose–lipid complex formation during cooking of rice flour. *Food Chemistry*, *71*, 511–517.

Kawai, K., Takato, S., Sasaki, T., & Kajiwara, K. (2012). Complex formation, thermal properties and in vitro digestibility of gelatinized potato–starch–fatty acid mixtures. *Food Hydrocolloids*, *27*, 228–234.

Le Bail, P., Buleon, A., Shiftan, D., & Marchessault, R. H. (2000). Mobility of lipid in complexes of amylose–fatty acids by deuterium and ^{13}C solid state NMR. *Carbohydrate Polymers*, *43*, 317–326.

Le Bail, P., Rondeau, C., & Buleon, A. (2000). Structural investigation of amylose complexes with small ligands, helical conformation, crystalline structure and thermostability. *International Journal of Biological Macromolecules*, *35*, 1–7.

Morrison, W. R. (1988). Lipids in cereal starches: A review. *Journal of Cereal Science*, *8*, 1–15.

Morrison, W. R., Tester, R. F., Snape, C. E., Law, R., & Gidley, M. J. (1993). Swelling and gelatinization of cereal starches. IV. Some effects of lipid-complexed amylase and free amylose in waxy and normal barley starches. *Cereal Chemistry*, *70*, 385–391.

Nebesny, E., Rosicka, J., & Tkaczk, M. (2005). Influence of selected parameters of starch gelatinisation and hydrolysis on stability of amylose–lipid complexes. *Starch-Starke*, *57*, 325–331.

North, A. M., Pethrick, R. A., & Wilson, A. D. (1978). Dielectric properties of phase separated polymer solids. 1. Styrene butadiene styrene triblock copolymers. *Polymer*, *19*(8), 913–922.

Ramasamy, P. (2012). A dielectric relaxation study of starch–water and starch–glycerol films. *Ionics*, *18*, 413–423.

Tang, M. C., & Copeland, L. (2007). Analysis of complexes between lipids and wheat starch. *Carbohydrate Polymers*, *67*, 80–85.

Tylianakis, M., Spyros, A., Dais, P., Taravel, F. R., & Perico, A. (1999). NMR study of the rotational dynamics of linear homopolysaccharides in dilute solutions as a function of linkage position and stereochemistry. *Carbohydrate Research*, *315*, 16–34.

Singh, N., Cairns, P., Morris, V. J., & Smith, A. C. (1998). Physical properties of extruded wheat starch-additive mixture. *Cereal Chemistry*, *75*, 325–330.

Shelat, K. J., Vilaplana, F., Nicholson, T. M., Gidley, M. J., & Gilbert, R. G. (2011). Diffusion and rheology characterisation of barley mixed linkage β glucan and possible implications for digestion. *Carbohydrate Polymers*, *86*, 1732–1738.

Snape, C. E., Morrison, W. R., Maroto-Valer, M. M., Karkalas, J., & Pethrick, R. A. (1998). Solid state C-13 NMR investigation of lipid ligands in V-amylose inclusion complexes. *Carbohydrate Polymers*, *36*(2–3), 225–237.

Waigh, T. A., Perry, P., Riekel, C., Gidley, M. J., & Donald, A. M. (1998). Chiral side-chain liquid-crystalline polymeric properties of starch. *Macromolecules*, *31*, 7980–7984.